Video Article

How to Quantify the Fraction of Photoactivated Fluorescent Proteins in Bulk and in Live Cells

Vanessa Chen[1], Malte Renz[1]

[1]Gynecologic Oncology Division, Stanford University School of Medicine

Correspondence to: Malte Renz at renzmalt@stanford.edu

URL: https://www.jove.com/video/58588
DOI: doi:10.3791/58588

Keywords: Photoactivatable fluorescent proteins, photoactivation efficiency, ratiometric intensity-based ensemble studies, photoconvertible fluorescent proteins, GFP, mCherry

Date Published: 12/20/2018

Citation: Chen, V., Renz, M. How to Quantify the Fraction of Photoactivated Fluorescent Proteins in Bulk and in Live Cells. *J. Vis. Exp.* (), e58588, doi:10.3791/58588 (2018).

Abstract

Photoactivatable and -convertible fluorescent proteins (PA-FPs) have been used in fluorescence live-cell microscopy for analyzing the dynamics of cells and protein ensembles. Thus far, no method has been available to quantify in bulk and in live cells how many of the PA-FPs expressed are photoactivated to fluoresce.

Here, we present a protocol involving internal rulers, *i.e.,* genetically coupled spectrally distinct (photoactivatable) fluorescent proteins, to ratiometrically quantify the fraction of all PA-FPs expressed in a cell that are switched on to be fluorescent. Using this protocol, we show that different modes of photoactivation yielded different photoactivation efficiencies. Short high-power photoactivation with a confocal laser scanning microscope (CLSM) resulted in up to four times lower photoactivation efficiency than hundreds of low-level exposures applied by CLSM or a short pulse applied by widefield illumination. While the protocol has been exemplified here for (PA-)GFP and (PA-)Cherry, it can in principle be applied to any spectrally distinct photoactivatable or photoconvertible fluorescent protein pair and any experimental set-up.

Video Link

The video component of this article can be found at https://www.jove.com/video/58588/

Introduction

In 2002, the first broadly applicable photoactivatable (PA-GFP[1]) and photoconvertible (Kaede[2]) fluorescent proteins were described. These optical highlighter fluorescent proteins change their spectral properties upon irradiation with UV-light, *i.e.,* they become bright (photoactivatable fluorescent proteins, *i.e.,* PA-FPs), or change their color (photoconvertible FPs). To date, several reversible and irreversible photoactivatable and photoconvertible fluorescent proteins have been developed[3,4]. In ensemble or bulk studies, optical highlighters have been used to study the dynamics of entire cells or proteins, and the connectivity of subcellular compartments. Furthermore, optical highlighters enabled single-molecule based superresolution imaging techniques such as PALM[5] and FPALM[6].

Although the photo*chemical* processes during photoactivation or -conversion have been described for many optical highlighters and even crystallographic structures before and after photoactivation/ -conversion have been made available[7,8], the underlying photo*physical* mechanism of photoactivation and -conversion is not completely understood. Furthermore, thus far only crude estimates exist of the efficiency of photoactivation and -conversion, that is, the fraction of fluorescent proteins expressed that is actually photoconverted or photoactivated to be fluorescent. *In vitro* ensemble studies have been reported quantifying the shift in absorption spectra and the amount of native and activated protein in a gel[9,10,11].

Here, we present a protocol involving fluorescent protein chimeras to assess the fraction of photoactivated fluorescent proteins in bulk and in live cells. Whenever working with genetically encoded fluorescent proteins, the absolute amount of protein expressed varies from cell to cell and is unknown. If one cell expressing a PA-FP shows a brighter signal after photoactivation than another cell, it cannot be differentiated if this brighter signal is due to higher expression of the PA-FP or a more efficient photoactivation of the PA-FP. To standardize the expression level in cells, we introduce internal rulers of genetically coupled spectrally distinct fluorescent proteins. By coupling the genetic information of a photoactivatable fluorescent protein to a spectrally distinct always-on fluorescent proteins, internal rulers are created that will still be expressed to an unknown total amount but in a fixed and known relative amount of 1:1. This strategy allows the quantitative characterization of different UV-light photoactivation schemes, *i.e.,* the assessment of the relative amount of PA-FPs that can be photoactivated with different modes of photoactivation, and thereby permits to define photoactivation schemes that are more effective than others. Furthermore, this strategy allows in principle the assessment of the absolute quantification of the photoactivated PA-FP fraction. To this end, it is important to realize that the presented ensemble studies are intensity-based which makes the analysis more complex as laid out in this protocol. Parameters determining the measured fluorescent intensity, *i.e.,* different molecular brightness, absorbance and emission spectra and FRET effects, need to be considered when comparing fluorescence intensities of different fluorescent proteins.

The presented ratiometric intensity-based quantification of photoactivation efficiency is exemplified for PA-GFP and PA-Cherry in live cells, but is in principle broadly applicable and can be used for any photoactivatable fluorescent protein under any experimental condition.

Protocol

1. Plasmid Construction

1. Generate two-color fusion probes. Use a mammalian cell expression vector (see **Table of Materials**) in which mCherry1[12] and PA-mCherry1[13] have been inserted with the restriction sites *AgeI* and *BsrGI*.
2. Order custom oligo-nucleotides to amplify the monomeric variants of eGFP and PA-eGFP containing the A206K mutation, *i.e.,* mEGFP and PA-mEGFP[14] without a stop codon as a *SalI-BamHI* fragment. Use the N-terminal primer 5'-AAT TAA CAG TCG ACG ATG GTG AGC AAG GGC GAG G 3' and the C-terminal primer 5'-AAT ATA TGG ATC CCG CTT GTA CAG CTC GTC CAT GC 3' and insert this *SalI-BamHI* fragment into the multiple cloning site of the expression vector. This will create the five amino acid linker RNPPV between the green and red fluorescent protein. We will refer to the fluorophore chimeras as GFP—Cherry, PA-GFP—Cherry, and GFP—PA-Cherry for the remainder of this article.
   Note: The coupling of fluorophores and creation of internal rulers to assess photoactivation efficiency can be done with any spectrally distinct fluorophore pair, *e.g.* superfolder PA-GFP [15]/ PA-TagRFP [16], *etc.* Many of the photoactivatable fluorescent proteins are derived from GFP. Hence, the primer sequence provided above can be used for many fluorescent proteins to construct a fluorophore chimera in a mammalian cell expression vector.

2. Cell Culture and Transfection

1. Use either any standard cell line such as HeLa, NRK, Cos-7 or a specific cell line to be used for specific photoactivation experiments. Use DMEM (supplemented with 10% fetal bovine serum, and 2 mM glutamine) and trypsin *without* phenol red (see **Table of Materials**) to reduce background fluorescence.
2. Detach the cells of a confluent culture with trypsin, count the number of cells in cell suspension using a Neubauer chamber, and seed 5,000 – 10,000 cells per well. Alternatively, use 1 drop from a 2-mL pipette of a 10-mL cell suspension from a confluent cell culture grown in a T 25-cell culture flask or 3 drops from a 5-mL cell suspension from a confluent culture grown in a T 12.5-cell culture flask.
3. Grow cells in 8-well chambers with #1.0 cover glass (see **Table of Materials**) for fluorescence live-cell microscopy.
4. Transfect cells 24 h after plating using commercial reagents (see **Table of Materials**) per distributer's protocol with the GFP—Cherry, PA-GFP—Cherry, and GFP—PA-Cherry chimeras.
5. Image cells after a total of 20 h post transfection to allow for protein expression, folding and maturation.

3. Imaging and Photoactivation

1. Image cells in a humidified and heated environmental chamber at 37 degrees Celsius. To buffer the cell media at physiological pH and render it CO_2-independent, add 20 mM HEPES, or use CO_2 gas set to 5% flow.
2. First, image cells expressing the GFP—Cherry construct. Set parameters that define time-integrated laser intensity per pixel in a confocal image, *i.e.,* pixel dwell time in microseconds, acousto-optical tunable filter (AOTF) transmission in percent, and digital zoom.
   Note: Using a 60x objective and a digital zoom of 3x allows imaging of a cell in its entirety while providing sufficient magnification. Set pixel dwell time to 2-4 µs and AOTF transmission for the 488-nm and 561-nm laser such that images show a good signal-to-noise ratio without any bleaching and no pixels indicating fluorescence intensity saturation.
3. Image, using the set laser power, AOTF transmission, pixel dwell time and digital zoom, 15-20 cells expressing GFP—Cherry.
4. Then, image with the same set laser power, pixel dwell time, AOTF transmission and digital zoom cells expressing GFP—PA-Cherry and PA-GFP—Cherry. Search for expressing cells in the green channel or red channel, respectively. Avoid long exposure of the cells during the search for expressing cells in order to not bleach the fluorescent proteins.
5. Set up a mini-time series with one pre-activation image and three post-activation images. The post-activation images will help identify potential transient dark states due to the exposure to UV-light.
   Note: In our hands, changes in detected fluorescence intensity due to transient dark states were <1% and could be neglected, but those dark states should be assessed for every experimental set-up.
6. To determine photoactivation efficiency, *i.e.,* the fraction of PA-FPs that is switched on to be fluorescent, in the specific photoactivation experiments that have already been established, apply the same photoactivation settings to 15-20 cells that are expressing the internal rulers introduced here and proceed with image analysis (section 4). If beginning to set up photoactivation experiments, find here a few different settings based on our experimental experience with PA-GFP and PA-Cherry; modify as needed.
   1. For instantaneous photoactivation of PA-GFP and PA-Cherry using a confocal laser scanning microscope (CLSM), apply 90 µW of 405-nm laser light in 3 or 5 iterations, respectively.
      Note: With our microscopic set-up, using a 38% AOTM transmission and a 2 µs pixel dwell time, we measured this 405-nm laser power in line-scan mode at the objective lens. With these settings, about 8% and 16% of the PA-GFP and PA-Cherry expressed can be photoactivated to be fluorescent. The entire titration series using CLSM for instantaneous photoactivation has been published previously[17].
   2. If a higher fraction of photoactivated PA-GFP and PA-Cherry fluorophores is advantageous *e.g.* to achieve a higher signal-to-noise ratio, and photoactivation does not have to be immediate, apply 40 µW of 405-nm laser light with a 2 µs pixel dwell time and 6% AOTF transmission for 450 iterations. Then, photoactivation will take up to 4 min as opposed to only 1-2 seconds, but photoactivation efficiency for PA-GFP will be 29% instead of 8%, allowing for a higher signal-to-noise ratio.
7. If a mosaic digital illumination system that contains micro mirror arrays in a spatial light modulator is available, 405-nm laser light can be used for widefield-photoactivation. This allows for efficient photoactivation within milliseconds.

Note: With 1.6 mW laser power as measured at the objective lens and an exposure time of 250 ms, 29% of PA-GFP can be photoactivated to be fluorescent.

8. Image with any set photoactivation parameters 15-20 cells expressing PA-GFP—Cherry and GFP—PA-Cherry, respectively.
9. Since pH, reactive oxygen species and other environmental factors may influence photoactivation efficiency, it may be important to assess photoactivation efficiencies of the PA-FPs in the respective subcellular micromilieu where the protein of interest is located. By coupling the fluorophore chimeras to the protein of interest, as the authors have done with the plasma membrane protein VSVG [18], photoactivation efficiency can be assessed in the specific subcellular compartment of interest.

4. Image Analysis and Algorithm for Ratiometric Intensity-based Quantification of Photoactivation Efficiency

1. Image analysis can be done with the open source image processing platforms ImageJ or Fiji. Determine the background fluorescence intensity in non-transfected cells in the green (B_1) and red (B_2) channel. Avoid perinuclear or any areas showing increased auto-fluorescence.
2. To determine the fluorescence intensity in a transfected cell, outline the cell body with the freehand selections tool. Again, avoid perinuclear or any other areas showing auto-fluorescence.
3. Subtract the background from the measured fluorescence intensity in each channel.
   $I_G = I_{Green\_measured} - B_1$
   $I_R = I_{Red\_measured} - B_2$
4. Use the GFP—Cherry construct to calculate the red-to-green ratio (RtoGr) and correct for donor-quenching due to fluorescence resonance energy transfer (FRET). The FRET efficiency E was determined to be 0.3 in previous experiments for the GFP—Cherry construct using the same amino acid linker between the two fluorophores[18].
   $RtoGr = (I_{Red\_measured} - B_2) / (I_{Green\_measured} - B_1)$
   $RtoGr_{corr} = RtoGr * (1 - E)$
   Note: In this intensity- based approach, donor quenching for mEGFP and PA-mGFP may be different given possible distinct spectral properties which have not been characterized. The rate of FRET (kET) and the Foerster distance (R0) depend upon the quantum yield of the donor which has not been determined for mEGFP and PA-mGFP.
5. Use the GFP—PA-Cherry construct to assess the fraction of photoactivated PA-Cherry. Determine the expected fluorescence intensity of PA-Cherry by multiplying the measured unquenched green fluorescence intensity of the GFP—PA-Cherry construct *prior* to photoactivation with the corrected red-to-green-ratio ($RtoGr_{corr}$).
   $I_{Red\_expected} = (I_{Green\_measured} - B_1) * RtoGr_{corr}$
   Note: As indicated above, the molecular brightness of the always-on FP and the photoactivatable FP may be different. See Discussion for more information on how to account for these differences.
6. Calculate the PA-Cherry photoactivation efficiency as a fraction of the measured red fluorescence intensity *after* photoactivation and the expected fluorescence intensity in the red channel.
   $(F_{PA\text{-}Cherry}) = (I_{Red\_measured} - B_2) / I_{Red\_expected}$
7. Use the PA-GFP—Cherry construct to assess the fraction of photoactivated PA-GFP. Determine the expected fluorescence intensity of PA-GFP by dividing the measured red fluorescence intensity of the PA-GFP—Cherry construct *prior* to photoactivation by the red-to-green-ratio (RtoGr). Here, the RtoGr does not need to be corrected for donor quenching, because GFP and PA-GFP are subject to donor quenching to the same amount.
   $I_{Green\_expected} = (I_{Red\_measured} - B_2) / RtoGr$
8. Calculate the PA-GFP photoactivation efficiency as a fraction of the measured green fluorescence intensity *after* photoactivation and the expected fluorescence intensity in the green channel.
   $(F_{PA\text{-}GFP}) = (I_{Green\_measured} - B_1) / I_{Green\_expected}$

Representative Results

The protocol presented here shows the ratiometric quantification of the fraction of fluorescent proteins that are photoactivated to be fluorescent (**Figure 1**). This fraction differs depending upon the mode of photoactivation.

A typical result using short time high-power photoactivation with a confocal laser scanning microscope (CLSM) is shown in **Figure 2c**. After titrating the laser power as measured at the objective lens by pixel dwell time and ATOF transmission, the maximum photoactivation efficiency for PA-GFP was about 8% and for PA-Cherry about 16%. The comparably low photoactivation efficiency of PA-GFP and PA-Cherry may be explained by simultaneous photoactivation and -destruction when exposed to a continuous deterministic stream of photons by CLSM. The shorter fluorescence lifetimes and the different, right-shifted absorption spectra of the red PA-FPs may contribute to the higher photoactivation efficiency of PA-Cherry compared to PA-GFP.

Using low laser power and hundreds of iterations, a higher photoactivation efficiency can be achieved. 450 iterations of UV-light delivered by a CLSM over a total of 4 min yielded a photoactivation efficiency of 29% for PA-GFP (**Figure 3c**). The higher photoactivation efficiency with repetitive exposure to UV-light photons may suggest a multi-step photoactivation process. Alternatively, the applied UV-light is strong enough to photoactivate but not enough to photodestruct which leads cumulative over time to a higher fraction of photoactivated fluorescent proteins.

With widefield illumination, the fluorophores are stochastically and repetitively exposed to 405-nm photons. Here, exposure for only 250 ms yielded a 29% photoactivation efficiency for PA-GFP.

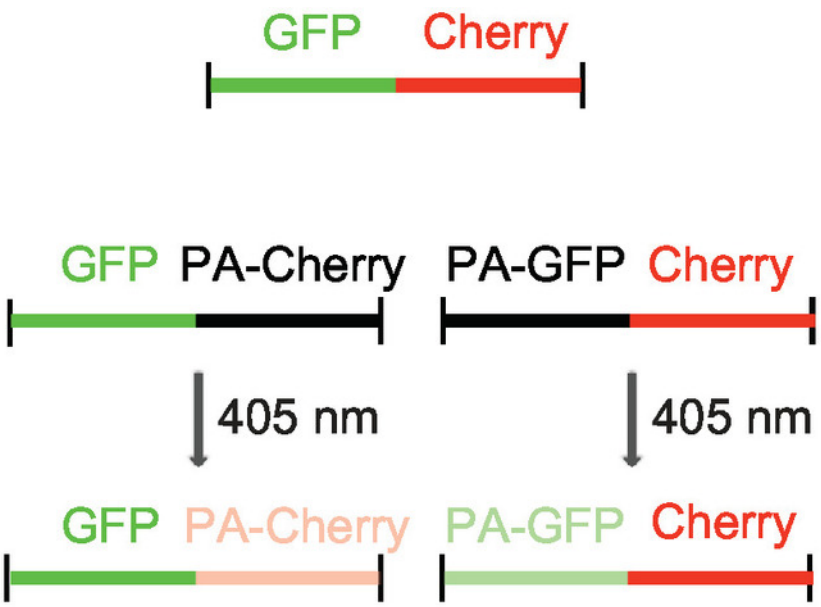

Figure 1: Concept of how to determine photoactivation efficiency in bulk and in live cells. By coupling spectrally distinct fluorescent proteins, internal rulers are created which allow for the ratiometric intensity-based assessment of photoactivation efficiency. Measured intensities of PA-Cherry and PA-GFP were related to expected intensities. Expected intensities were derived from determining the fluorescence intensity of the always-on fluorescent proteins in the GFP-Cherry, GFP-PA-Cherry or PA-GFP-Cherry chimeras prior to photoactivation. Figure modified from Renz and Wunder 2017[17]. Please click here to view a larger version of this figure.

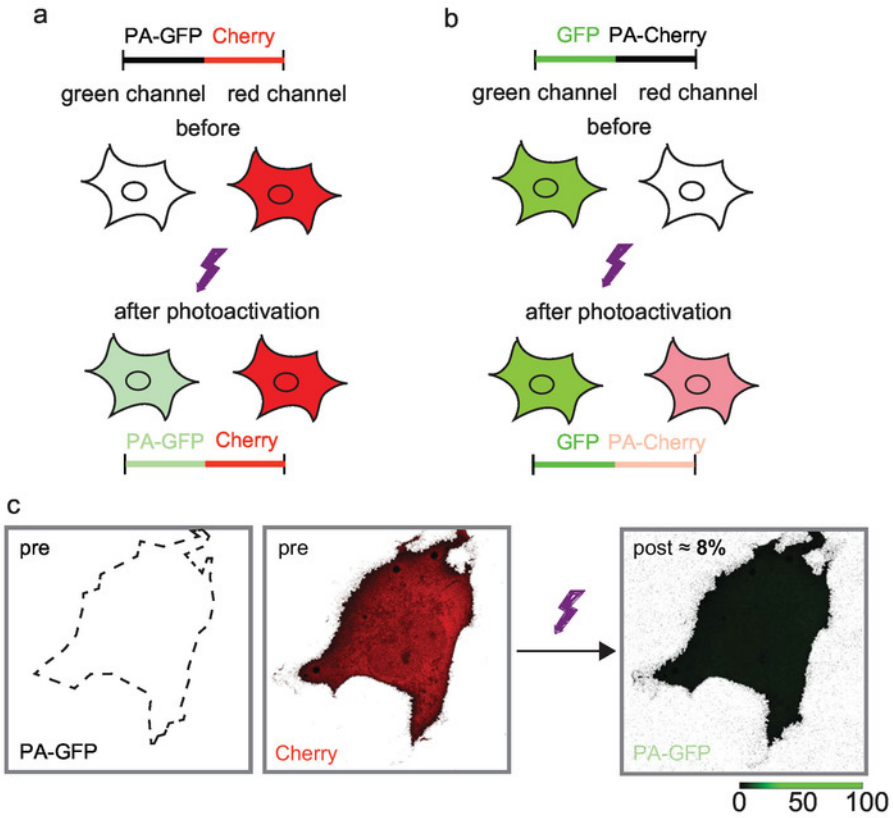

Figure 2: Bulk photoactivation of PA-GFP-Cherry (a) and GFP-PA-Cherry (b) as instantaneously and completely as possible using a confocal laser-scanning microscope in live cells. 8% of PA-GFP expressed was photoactivated with a pixel dwell time of 2 µs and an AOTF transmission of 38% which result in laser power of 90 µW, as measured at the objective lens and 3 iterations (c). Increasing the 405-nm laser power did not increase photoactivation efficiency. Figure modified from Renz and Wunder 2017[17]. Please click here to view a larger version of this figure.

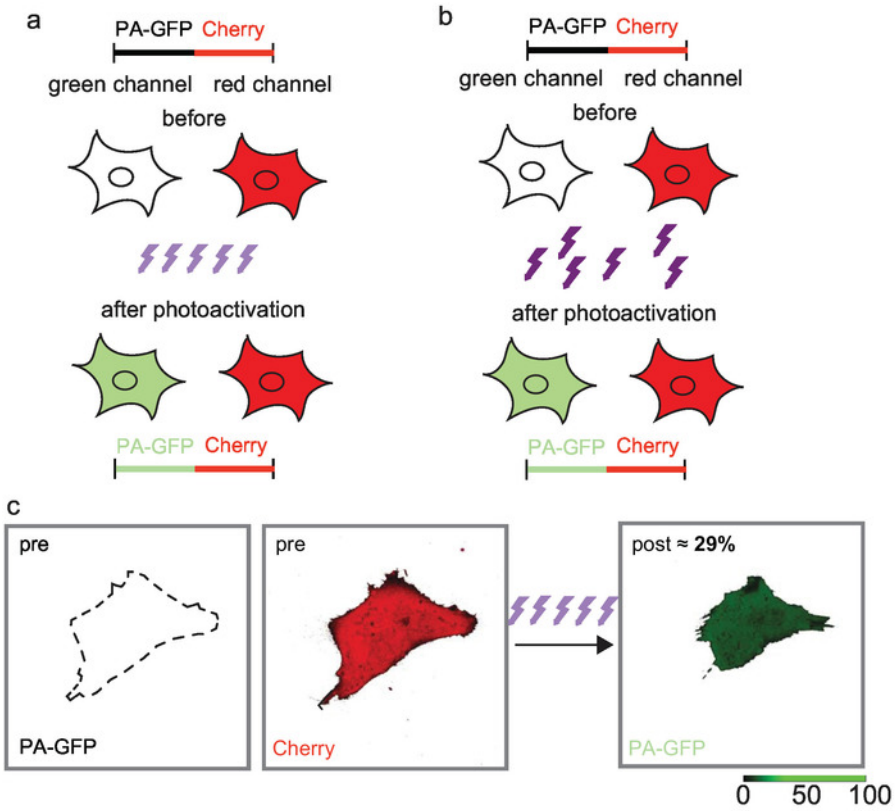

Figure 3: Iterative low-power photoactivation with a confocal laser-scanning microscope (a) and short high-power widefield illumination (b) yield higher photoactivation efficiencies. 29% of PA-GFP was photoactivated with a pixel dwell time of 2 µs and an AOTF transmission of 6%, which result in laser power of 40 µW, as measured at the objective lens and 450 iterations (c). Figure modified from Renz and Wunder 2017[17]. Please click here to view a larger version of this figure.

Discussion

So far, no method existed to determine in bulk the fraction of PA-FPs expressed in live cells that is photoactivated to be fluorescent. The presented protocol can be used for any spectrally distinct fluorescent protein pair. While exemplified here for the irreversible PA-FPs PA-GFP and PA-Cherry, this approach is in principle applicable to photoconvertible proteins as well. The spectrally distinct fluorescent protein, however, must be selected carefully to minimize spectral overlap given that photoconvertible fluorescent proteins shift their absorbance and emission spectra, *e.g.* from green to red fluorescence.

As outlined above, it is important to state that the presented approach is ratiometric and intensity-based. It can be used to standardize the unknown expression level in cells and define relative differences in photoactivation efficiency by different modes of photoactivation. The protocol can also be used to assess the absolute fraction of photoactivated PA-FPs. Then, different spectral properties of different FPs need to be taken into account.

The molecular brightness (MB) is the product of quantum yield (QY), extinction coefficient (EC) and percent absorbance at the given excitation wavelength relative to the absorbance peak. For Cherry[12] and PA-Cherry[13], respective values of QY and EC have been published. The percent absorbance at the given excitation wavelength of 543 nm relative to absorbance peak is 0.5 and 0.7, respectively.
MB_{Cherry} = 0.22 * 72,000 * 0.5 = 7,920
$MB_{PA\text{-}Cherry}$ = 0.46 * 18,000 * 0.7 = 5,796
Thus, the lower molecular brightness of PA-Cherry compared to Cherry can be taken into account by dividing $I_{Red\_expected}$ by 1.37 (derived from 7,920/5,796).

However, it is unknown under which photoactivation conditions the published molecular brightness of PA-Cherry has been determined. This is important, since we show here that the mode of photoactivation changes the measured fraction of photoactivated PA-FPs. Furthermore, for the monomeric versions comprising the A206K mutation. *i.e.,* mEGFP and PA-mEGFP, no molecular brightness has been published.

In this ratiometric intensity-based approach, the molecular brightness of the PA-FPs and the always-on FP counterparts in a first approximation have been considered identical. We decided on this approach, since (i) for some FPs no molecular brightness has been reported, and (ii) it is thus far unclear in how far different modes of photoactivation may affect the molecular brightness of the PA-FPs reported in the literature. Furthermore, (iii) for a comparative analysis the knowledge of the molecular brightness is not necessary; it is only needed for the intensity-based determination of the absolute fraction of photoactivated PA-FPs which can be calculated as shown above.

Our approach involving fluorescent protein chimeras as internal rulers shows that different exposure to UV-light yields different photoactivation efficiencies. Thereby, it defines options as how to photoactivate a larger PA-FP fraction and achieve a better signal-to-noise ratio. Furthermore,

it opens up opportunities to differentially photoactivate different PA-FPs in the same cell given their differential response to UV-light or to differentially photoactivate the same PA-FP in different subcellular compartments by exposing it differently to UV-light. In summary, our protocol will help further the quantitative understanding of cellular processes using PA-FPs in live-cell microscopy.

Disclosures

The authors have nothing to disclose.

Acknowledgements

We would like to thank the Dorigo laboratory and the Neuroscience Imaging Service at Stanford University School of Medicine for providing equipment and space for this project.

References

1. Patterson, G. H., & Lippincott-Schwartz, J. A photoactivatable GFP for selective photolabeling of proteins and cells. *Science.* **297** (5588), 1873-1877, (2002).
2. Ando, R., Hama, H., Yamamoto-Hino, M., Mizuno, H., & Miyawaki, A. An optical marker based on the UV-induced green-to-red photoconversion of a fluorescent protein. *Proceedings of the National Academy of Sciences of the United States of America.* **99** (20), 12651-12656, (2002).
3. Renz, M., & Lippincott-Schwartz, J. in *The Fluorescent Protein Revolution Series in Cellular and Clinical Imaging.* eds R. N. Day & M. W. Davidson Ch. 9, 201-228 CRC Press (2014).
4. Shcherbakova, D. M., Sengupta, P., Lippincott-Schwartz, J., & Verkhusha, V. V. Photocontrollable fluorescent proteins for superresolution imaging. *Annual Review of Biophysics.* **43** 303-329, (2014).
5. Betzig, E. *et al.* Imaging intracellular fluorescent proteins at nanometer resolution. *Science.* **313** (5793), 1642-1645, (2006).
6. Hess, S. T., Girirajan, T. P., & Mason, M. D. Ultra-high resolution imaging by fluorescence photoactivation localization microscopy. *Biophysical Journal.* **91** (11), 4258-4272, (2006).
7. Henderson, J. N. *et al.* Structure and mechanism of the photoactivatable green fluorescent protein. *Journal of the American Chemical Society.* **131** (12), 4176-4177, (2009).
8. Subach, F. V. *et al.* Photoactivation mechanism of PAmCherry based on crystal structures of the protein in the dark and fluorescent states. *Proceedings of the National Academy of Sciences of the United States of America.* **106** (50), 21097-21102, (2009).
9. Wiedenmann, J. *et al.* EosFP, a fluorescent marker protein with UV-inducible green-to-red fluorescence conversion. *Proceedings of the National Academy of Sciences of the United States of America.* **101** (45), 15905-15910, (2004).
10. Habuchi, S., Tsutsui, H., Kochaniak, A. B., Miyawaki, A., & van Oijen, A. M. mKikGR, a monomeric photoswitchable fluorescent protein. *PLoS One.* **3** (12), e3944, (2008).
11. McKinney, S. A., Murphy, C. S., Hazelwood, K. L., Davidson, M. W., & Looger, L. L. A bright and photostable photoconvertible fluorescent protein. *Nature Methods.* **6** (2), 131-133, (2009).
12. Shaner, N. C. *et al.* Improved monomeric red, orange and yellow fluorescent proteins derived from Discosoma sp. red fluorescent protein. *Nature Biotechnology.* **22** (12), 1567-1572, (2004).
13. Subach, F. V. *et al.* Photoactivatable mCherry for high-resolution two-color fluorescence microscopy. *Nature Methods.* **6** (2), 153-159, (2009).
14. Zacharias, D. A., Violin, J. D., Newton, A. C., & Tsien, R. Y. Partitioning of lipid-modified monomeric GFPs into membrane microdomains of live cells. *Science.* **296** (5569), 913-916, (2002).
15. Slocum, J. D., & Webb, L. J. A Double Decarboxylation in Superfolder Green Fluorescent Protein Leads to High Contrast Photoactivation. *Journal of Physical Chemistry Letters.* **8** (13), 2862-2868, (2017).
16. Subach, F. V., Patterson, G. H., Renz, M., Lippincott-Schwartz, J., & Verkhusha, V. V. Bright monomeric photoactivatable red fluorescent protein for two-color super-resolution sptPALM of live cells. *Journal of the American Chemical Society.* **132** (18), 6481-6491, (2010).
17. Renz, M., & Wunder, C. Internal rulers to assess fluorescent protein photoactivation efficiency. *Cytometry A.* (2017).
18. Renz, M., Daniels, B. R., Vamosi, G., Arias, I. M., & Lippincott-Schwartz, J. Plasticity of the asialoglycoprotein receptor deciphered by ensemble FRET imaging and single-molecule counting PALM imaging. *Proceedings of the National Academy of Sciences of the United States of America.* **109** (44), E2989-2997, (2012).

